Pump−Deplete−Probe Spectroscopy and the Puzzle of Carotenoid Dark States

Wendel Wohlleben,[†] Tiago Buckup,[†] Hideki Hashimoto,[§] Richard J. Cogdell,[¶] Jennifer L. Herek,[‡] and Marcus Motzkus*,[†]

Max-Planck-Institut für Quantenoptik, 85748 Garching, Germany, Department of Physics, Osaka City University, Osaka 558-8585, Japan, Institute of Biomedical and Life Sciences (IBLS), University of Glasgow, Glasgow G12 8QQ, United Kingdom, and FOM−Institute for Atomic and Molecular Physics, 1098 SJ Amsterdam, The Netherlands

Received: July 23, 2003; In Final Form: January 12, 2004

Pump−deplete−probe and transient absorption spectroscopy are applied to carotenoids with $N = 11$ conjugated double bonds in solution to study the origin of recently observed transient features that have been previously assigned to new electronic states. The depletion pulse pumps the transient near-IR band, whose lifetime coincides with the fluorescence lifetime, and is hence attributed to the S_2 state. The subsequent signal of any lower-lying dark excited-state populated by internal conversion from S_2 should be affected by the depletion pulse. Correspondingly, the signal in the S_1 deactivation channel is diminished by the depleted excited population. In contrast, the S_{sol}* signal, purportedly reflecting an intermediate state on a competing deactivation pathway, is not affected by the depletion pulse. When comparing our results with literature data for other carotenoids, we find that the S_{sol}* lifetime is constant at 6.2 ± 0.4 ps for any $N \geq 11$ carotenoid; for shorter chain lengths, it is equal to the S_1 lifetime. To explain this puzzle, S_{sol}* is identified as a vibrationally excited ground state (S_{sol}* = hot S_0), populated by a combination of impulsive Raman scattering of the pump pulse and internal conversion (S_1-S_0), and decaying by vibrational relaxation. The S_{sol}* state is not identical to the S_T* state, which appears in the same spectral region when the carotenoid is embedded in light-harvesting complexes.

1. Introduction

Numerous recent experiments of the deactivation energy flow in photoexcited carotenoids have focused on the existence and possible role of dark states. The linear absorption spectrum of carotenoids contains only one bright state, conventionally labeled S_2 or $1B_u^+$ in the idealized linear C_{2h} symmetry.[1] The traditionally accepted mechanism of deactivation from S_2 involves internal conversion to the dark S_1 ($2A_g^-$) state, which is one-photon-forbidden from the ground-state S_0 ($1A_g^-$). The S_1 decay to the ground state follows the energy-gap law[2] of weak vibronic interaction quite well.[3−5] However, calculations with full configuration interaction indicate that below S_2, there exists not one but, depending on the conjugation length, up to three dark states.[6] The group of Koyama and co-workers identified the energetic positions of $2A_g^-$, $1B_u^-$, and $3A_g^-$ from resonance Raman profiles.[7] These findings have inspired several conflicting proposals that were focused on identifying certain spectral dynamics in the deactivation of S_2 with these dark states. Recently, the early spectral dynamics related to fast near-IR bands have been ascribed to the $1B_u^-$ and $3A_g^-$ states as intermediates along the pathway to the $2A_g^-$ (S_1) state.[8,9]

In this contribution, we focus on the so-called S* band that is found in carotenoids, which is characterized by a transient absorption signal on the lower-energy side of the S_0-S_2 absorption.[10−12] For clarity, we label the signal observed for carotenoids in solution[10,11] as S_{sol}*. For carotenoids in light-harvesting (LH) complexes, there is further evidence of ultrafast singlet−triplet conversion within the carotenoid[12,13] that proceeds via the S* state. We distinguish this situation by labeling the carotenoid state in LH complexes as S_T* and note that, in previous work, it was also attributed to the $1B_u^-$ state.[12,13] The lack of an unified picture of carotenoids deactivation is ultimately unsatisfying. Does an alternative deactivation channel S* exist? Is it the same for carotenoids in solution and in LH complexes? What is the nature of the spectral dynamics during the fluorescence lifetime?

The quantum theory of polyenes with up to $N = 4$ conjugated double bonds provides paramount evidence that the deactivation of S_2 is governed by strong vibronic interaction, which leads to real crossings of the electronic surfaces.[14] Although explicit calculations for biologically relevant carotenoids ($N > 9$) are beyond present computing power, there is no reason to assume that this mechanism would be different. Thus, rather than contemplate the S_2-S_1 energy gap, we should imagine a wave packet moving on the S_2 potential energy surface to a point where nuclear symmetry deformation induces degeneracy of the upper and lower electronic states such that their surfaces form a conical intersection.[15] To characterize the dynamical network of excited states, the use of a second pump (depletion) beam that manipulates the excited-state population is a powerful method and previously has been applied successfully on rhodopsin.[16]

Here, we report pump−deplete−probe and transient absorption experiments on $N = 11$ carotenoids in solution. We find that the lifetime of S_{sol}* is the same for $N = 11-19$ and, for $N < 11$, is equal to the S_1 lifetime. By analysis of the depletion experiments, we identify the S_{sol}* signal as the Raman-excited

* Author to whom correspondence should be addressed. E-mail: mcm@mpq.mpg.de.
[†] Max-Planck-Institut für Quantenoptik.
[§] Osaka City University.
[¶] IBLS, University Glasgow.
[‡] FOM−Institute for Atomic and Molecular Physics.

10.1021/jp036145k CCC: $27.50
Published on Web 02/11/2004

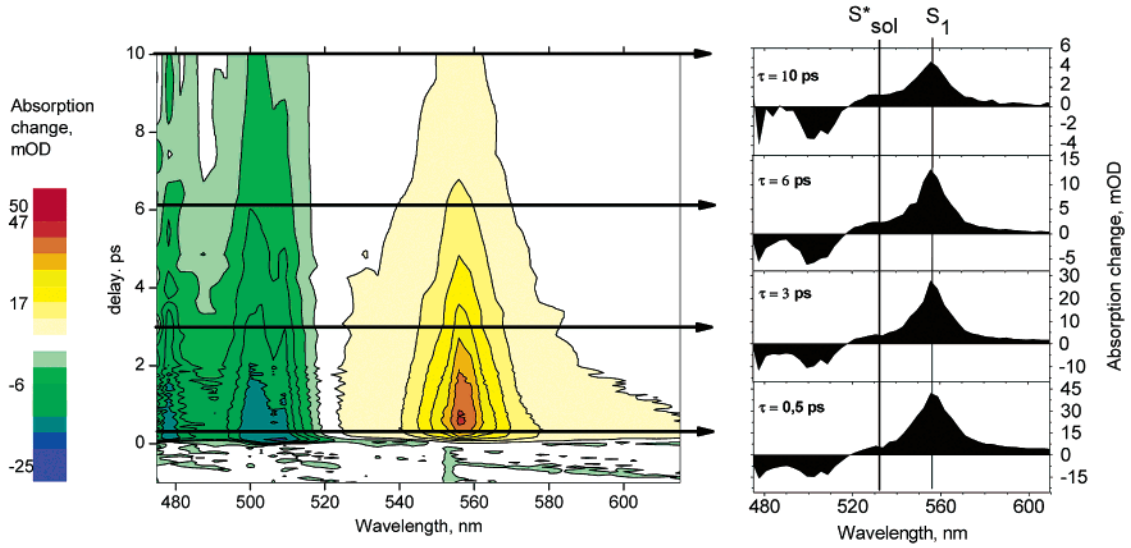

Figure 1. Transient absorption of lycopene. Features are the peak of S_1 absorption at 555 nm with initial vibrational cooling on the red side (~580 nm), the bleach of ground-state S_0-S_2 (0−0) absorption at 500 nm, and, on its red side, the S_{sol}* absorption, which lives slightly longer than S_1. Vertical lines in the spectral cuts (right-hand side of figure) define the positions of the S_{sol}* and S_1 signals.

ground state: S_{sol}* = hot S_0, as has been suspected by Andersson and Gillbro.[10] We further provide evidence that the characteristics of the ~200-fs Franck−Condon windows of depletion (this work), absorption,[9] and fluorescence[17] are all linked to wave-packet motion on the S_2 potential energy surface, as supported by theory.[18]

2. Materials and Methods

Sample Preparation. All-*trans*-β-carotene was purchased from Sigma−Aldrich and was used as received. All-*trans*-zeaxanthin was graciously given to us by Tomáš Polívka (Lund Universitet) and was originally a gift from Hoffman−LaRoche. All-*trans*-lycopene was extracted from tomato and refined by chromatography by co-authors H.H. and R.J.C. Lycopene and β-carotene were dissolved in *n*-hexane; zeaxanthin was dissolved in methanol. The solution was prepared fresh everyday and placed in the cell under a nitrogen atmosphere, to avoid sample oxygenation. The samples had a maximum absorption of 0.25−0.35 OD and were held in a 0.2-mm-thick sealed rotating cell at room temperature.

Conventional Transient Absorption Measurements. The setup has been described previously.[12] In short, a home-built 1 kHz noncollinear optical parametric amplifier generates the pump beam, centered at 505 nm for lycopene and at 490 nm for β-carotene and zeaxanthin, with a pulse duration of 33 fs. This excitation is selective for the 0−0 transition on the S_2 state. The white-light continuum probe beam was detected using a photomultiplier in conjunction with a monochromator, with a spectral resolution of 3 nm. The time dispersion in the white light was compensated automatically, after a prior calibration, with a computer-controlled delay line synchronized to the monochromator steps. Every transient absorption spectrum is the average of 15 scans of 100 shots per point.

Ultrafast Pump−Deplete−Probe Spectroscopy. In this technique, a fraction of the fundamental light from our femtosecond laser (center wavelength of 795 nm and pulse duration of 110 fs) is added as a second pump, or "depletion" pulse, with variable delay. The response function is now given by the cross-correlation between the pump and the depletion pulse (~120 fs). The zero-delay point between the white light and the visible pump pulse was determined using the instantaneous bleach signal at ~500 nm, whereas the zero-delay point between the depletion and the white light probe was determined using the off-resonant mixing signal of the depletion pulse with the white light.

All beams were focused and superimposed in the sample with concave mirrors. The pump was attenuated to pulse energies of <70 nJ with a focal spot diameter of 280 μm, or 2.8×10^{14} photons/cm^2. The depletion pulse was 1.7 μJ strong at a focal spot diameter of 340 μm, or 7.5×10^{15} photons/cm^2. The probe beam had a diameter of 74 μm such that the probed volume was of homogeneous pump intensity. Only when we measured power dependencies of the depletion effect it occurred that the samples were permanently bleached at depletion energies around 4 μJ. For all measurements presented here, we stayed well below that threshold and checked carefully that the samples showed no signs of degradation.

3. Transient Absorption

Results. The time-wavelength resolved absorption of lycopene ($N = 11$) is displayed in Figure 1. The region that has been proposed to reflect the $S^*/1B_u^-$ signal is the positive absorption on the red side of the ground-state absorption (here, at ~535 nm). Indeed, this absorption, termed here as S_{sol}*, has more weight, compared to S_1 at longer delays (see Figure 1, right). However, there is no signal that survives hundreds of picoseconds, excluding the population of the triplet T_1. To link the situation in solution to the carotenoid incorporated in LH2 directly, we apply the same rate equation model that turned out to be the best in LH2.[12] Therefore, we optimize the model parameters—conversion rates and spectral profiles—with an evolutionary target analysis of the 2D data.[12] The model lets S_2 decay via two competing channels, to S_{sol}* and S_1, which can then interconvert, as well as relax further to S_0 (Figure 2c). The optimal fit nicely separates the two contributions, both of which have approximately Gaussian shape, with additional contributions of the vibrationally hot S_1 state and ground-state bleach (Figure 3a). The bands are broader in zeaxanthin and β-carotene (Figure 3b), because of the contribution of the cyclic end groups to the conjugation system, which is identical for the two carotenoids and renders them spectroscopically interchangeable.[19] In the optimal model parameters, the conversion

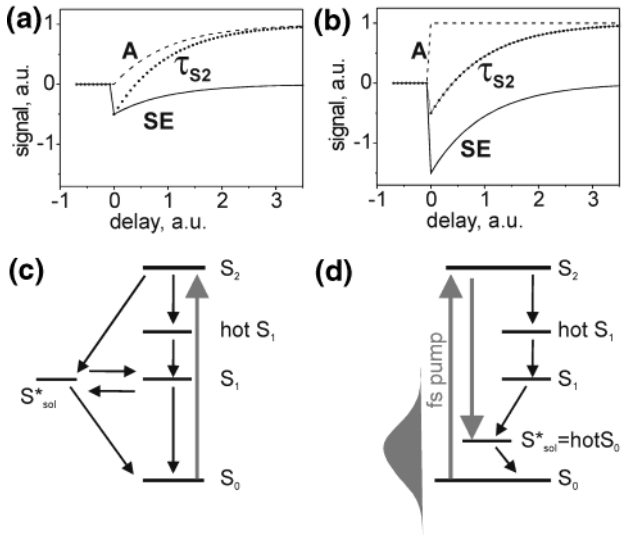

Figure 2. Models of energy flow: (a) transient absorption (A) rises with τ_{S_2}, whereas stimulated emission (SE) decays with τ_{S_2} (the sum displays the time constant τ_{S_2}); and (b) absorption A rises instantaneously, whereas SE decays with τ_{S_2} (the sum signal (symbols) is indistinguishable from the sum signal of panel a (solid curve through symbols)). Panel c shows the "$1B_u^-$ hypothesis", where S_{sol}* is an excited state, possibly identical with S_T* ($1B_u^-$, and panel d shows the "ground-state hypothesis", where S_{sol}* is hot S_0 and is not identical to S_T*.

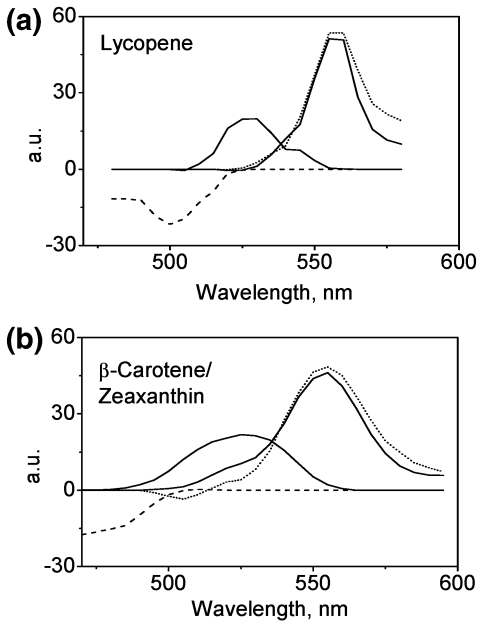

Figure 3. Target spectra from a global analysis of time-wavelength-resolved transient absorption: (a) lycopene and (b) β-carotene and zeaxanthin. The results for β-carotene and zeaxanthin are practically identical. The spectra of S_{sol}* (solid line, 530 nm) and S_1 (solid line, 560 nm) are well distinguished. Additional contributions come from hot S_1 (dotted line) and ground-state bleach (dashed line).

from S_{sol}* to S_1 is <2% and the S_1 to S_{sol}* conversion is <10%. Similar data were acquired on zeaxanthin and β-carotene (data not shown). By comparing the ground-state absorption spectrum of β-carotene ($N = 11$, cyclized) with the absorption spectra of lycopene ($N = 11$, linear) and spheroidene ($N = 10$, linear),[5] we attributed an effective conjugation length of 10.1 to β-carotene, in accord with the value of 9.8 that was derived from fluorescence.[20] Similar corrections are, for our purposes, not critical for the other carotenoids and, hence, are omitted. The lifetimes from monoexponential fits at the S_1 (560 nm) and S_{sol}* (535 nm) bands provide the stunning result that the lifetime of S_{sol}* is the same for any carotenoid with $N \geq 11$ (Figure 4). The S_{sol}* lifetime seems to mimick the lifetime of S_1 for $N <$ 11.

In a more-detailed analysis, the kinetics of S_1 in lycopene at 560 nm (Figure 5a) show two rise times: 100 ± 30 fs and 450 ± 100 fs. The decay is monoexponential, with 4.2 ± 0.2 ps. These values agree well with previous studies.[9,19] The rise times can be attributed to the S_2-S_1 internal conversion and the slower vibrational cooling in S_1. The decay is caused by the S_1-S_0 internal conversion. The kinetics at the S_{sol}* probe wavelength of 535 nm are complicated by the overlap with stimulated emission (SE) from S_2 (Figure 5b). We assume an instantaneous rise of the negative contribution from stimulated emission and extract two rise times toward positive absorption: 70 ± 30 fs and 250 ± 100 fs. The decay of S_{sol}* is 5.8 ± 0.2 ps, significantly slower than that of S_1. We note that the ratio of signal amplitudes (S_{sol}*/S_1) is dependent on excitation wavelength, as will be published elsewhere.[21]

The transients on β-carotene and zeaxanthin (not shown here) are qualitatively the same as in lycopene. Rise times of S_1 are 150 ± 30 fs in both carotenoids, which is in reasonable agreement with β-carotene fluorescence lifetimes of 180 ± 15 fs (from Akimoto et al.[17]) or 195 ± 15 fs (from Macpherson and Gillbro[22]). Additional slower rise times of ~500 fs from vibrational cooling are in accord with previous measurements.[19] The rise time of S_{sol}*, which is again obstructed by SE, is 165 ± 30 fs. The decay of S_1 is 9.3 ± 0.4 ps, as measured previously,[19] and the decay of S_{sol}* is almost the same (10.1 ± 0.6 ps).

Discussion. The phenomenon of an absorption signal that lives longer than S_1 and that is located on the lower-energy (red) side of ground-state absorption has been observed previously: In $N = 15$ and $N = 19$, this signal has been attributed to the absorption of the hot ground state.[10] The charm of this attribution is that it rationalizes the spectral position of the S_{sol}* signal, which would be the naturally red-shifted hot S_0-S_2 band. In $N = 13$, the S_{sol}* signal was identified with an excited state.[11] For $N = 11$ and shorter, an independent absorption band has never been identified in the S_{sol}* region.

It is well-known that, for conjugated systems, the energies of excited states scale with conjugation length. We fit the S_1 lifetime in the form of the energy-gap law[2] with an inverse energy scaling with conjugation length, because this is the least-speculative expansion:

$$\tau_{S_1}^{-1} = P_1 \exp\left[\frac{(P_2/N) + E_\infty}{\hbar\omega_{acc}/\gamma}\right] \qquad (1)$$

This procedure is not meant to be a determination of energies, but rather to identify the mechanism of excited-state deactivation. We fix $E_\infty = 3500\ cm^{-1}$, $\gamma = 1$, and $\hbar\omega_{acc} = 1500\ cm^{-1}$. Best-fit parameters are then $P_1 = 2.5 \times 10^4\ ps^{-1}$ and $P_2 = 1.5 \times 10^5\ cm^{-1}$ (see solid curve in Figure 4). In comparison, the lifetimes of S_{sol}* do not exhibit the expected exponential dependence on N and, hence, do not obey the energy-gap law. Taken together, all measurements of carotenoids with $N \geq 11$ yield an average S_{sol}* lifetime of 6.2 ± 0.4 ps. The constant lifetime of S_{sol}* for $11 \leq N \leq 19$ raises serious doubt as to whether S_{sol}* can be the signal of an electronically excited state.

We will now discuss possible models of energy flow, aided by simple simulations of kinetics traces. Consider again the "$1B_u^-$ hypothesis" shown in Figure 2c. If an excited-state S_{sol}*

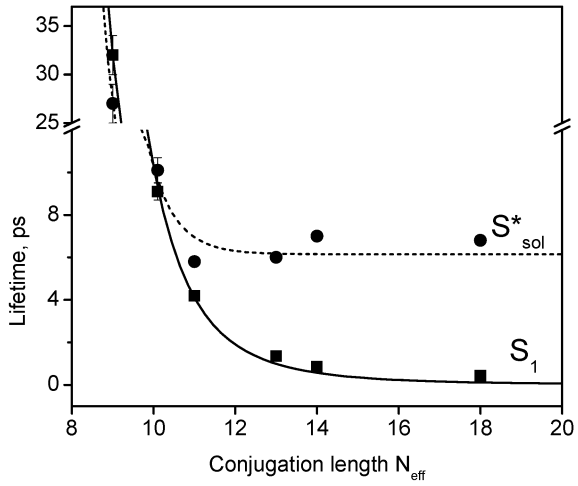

Figure 4. Lifetimes of S_1 and S_{sol}*. Combined plot of $N = 10.1$ and 11 (this work), with $N = 13$ (from ref 11), $N = 15$ and 19 (from ref 10), and $N = 9$ (from ref 21). The dotted curve is a guide to the eye for S_{sol}*, and the solid curve is a fit using the energy-gap law for S_1.

is populated from S_2, then its absorption (A) should increase with the same time constant as the decay of the S_2 state (τ_{S_2}), which is observable via its SE (see Figure 2a). In the special case of S_{sol}*, both A and SE contribute at the same wavelength; therefore, only the sum signal is detected in the kinetics, with a single time constant τ_{S_2} in the rise. However, the case illustrated in Figure 2b shows how an identical kinetic signal can be generated by an SE signal that again decays with τ_{S_2} and an absorption A that now appears instantaneously. Such kinetics are expected for the model in Figure 2d, in which a Raman process instantaneously populates the hot ground state. Evidence for this "ground-state hypothesis" will be given in more detail below. The model of Figure 2d rationalizes both the spectral position of S_{sol}* and its constant lifetime (see Figure 4), which now is attributed to ground-state vibrational relaxation. In this model, the hot ground state would be populated both by the pump pulse and later on by the delayed S_1-S_0 internal conversion; therefore, its lifetime would never drop below that of S_1, as measured in Figure 4.

On the basis of the simple simulations of kinetics traces (Figure 2), we stress that, in the special case of spectral overlap with SE from the precursor S_2, a transient absorption experiment cannot discriminate a priori between the two models.

4. Pump−Deplete−Probe Spectroscopy

To characterize the deactivation network of states, we manipulate the population of one state and observe how signals from other states change concomitantly (or not). After excitation, a comparably strong pulse, adapted in time and wavelength to the Franck−Condon window of a specific state, depletes some of its population. All states that arise via the decay of this depleted state will hence suffer the same depletion. Here, we choose the transient near-IR band of carotenoids as the depletion resonance. Because the lifetime of this signal[8] is equal to the fluorescence lifetime,[22] we assume that the absorbing state is S_2, because S_2 is the only bright state of the excited manifold (alternative interpretations will be discussed below). Guided by the S_2 IR absorption spectrum, the depletion pulse takes the population to very high-lying singlet states and probably to the radical cation. The cation absorption signal is known to be positive in the IR region and virtually zero in the visible region,[23] thus minimizing artifacts at wavelengths where we probe the S_{sol}* and S_1 dynamics.

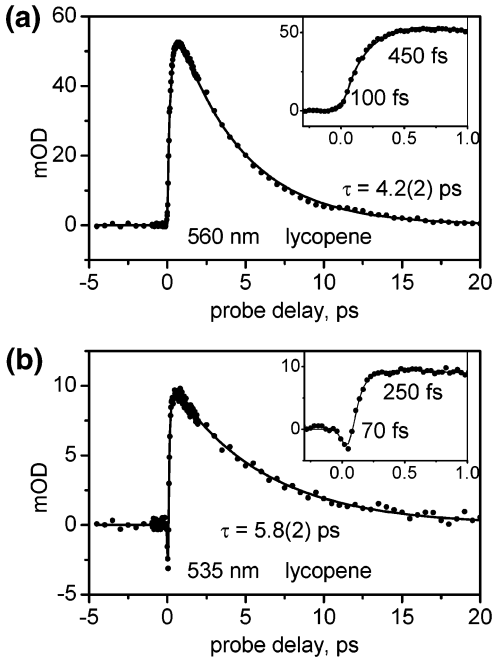

Figure 5. Kinetics in lycopene: (a) S_1 (560 nm) and (b) S_{sol}* (535 nm), showing significantly longer lifetime. The insets zoom into the first picosecond of the kinetics. Lines are multiexponential fits, convoluted with the experimental resolution.

Results. The pump−probe delay is fixed at $t_{probe} = 2$ ps, which is approximately half the S_1 lifetime in lycopene. In addition, the depletion pulse comes at a pump−deplete delay of $T = 50$ fs, which is well in the near-IR band window.[8] The presence of the depletion pulse diminishes the S_1 absorption, as measured 2 ps later, by ∼15%, but does not affect the S_{sol}* absorption (Figure 6a). The S_{sol}* signal is not sensitive to the presence of the depletion pulse. The same effect is observed in zeaxanthin and β-carotene (data not shown).

Continuing with lycopene, we now set the detection wavelength to $S_1 = 560$ nm and scan the pump−deplete delay while still detecting at a pump−probe delay of 2 ps. A short-lived resonance is seen (Figure 6b), as expected for the fast, near-IR bands. The curve is fitted with a monoexponential rise and decay, convoluted with the pump−deplete cross-correlation of 110 fs. The rise time and/or delay from time zero are not resolved and, hence, are estimated to be <20 fs. The majority of the signal decays in 110 ± 30 fs, to a weaker asymptotic depletion effect for long pump−deplete delays ($T >$ 300 fs). We stress that for any delay, exclusively the S_1 absorption is affected and never the S_{sol}* band.

If we vary the energy of the depletion pulse, the signal in the region of the peak at 50 fs scales linearly with energy, whereas the asymptotic region scales in a nonlinear fashion (Figure 7a). Interestingly, also the lifetime of the peak changes (see Figure 7b). With higher energy, it rises approximately linearly until reaching a maximum of 195 ± 15 fs in zeaxanthin at a threshold energy of ∼2 μJ, or 9×10^{15} photons/cm^2.

To summarize the key result of the pump−deplete−probe experiments, we find that, upon depletion of S_2 population, only the S_1 signal is affected. This immediately leads to the conclusion that S_{sol}* is not identical to either S_2 or S_1.

Discussion of Bright-State Dynamics. The maximum lifetime of the depletion signal measured in zeaxanthin or β-carotene is 195 ± 15 fs and may be compared quantitatively to the reported fluorescence lifetime of β-carotene of 177 ± 10 fs (from Macpherson and Gillbro[22]) or 195 ± 10 fs (from Kandori

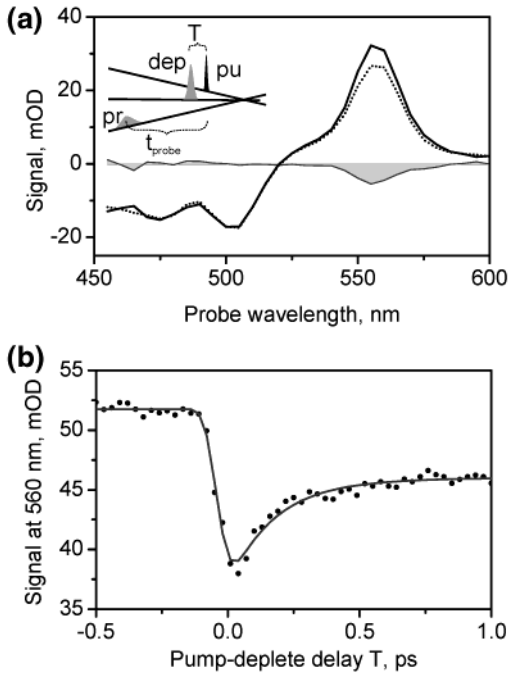

Figure 6. Pump−deplete−probe in lycopene: (a) transient absorption spectrum at $t_{probe} = 2$ ps without depletion (solid line) and with depletion ($T = 50$ fs) after excitation (dotted line). The difference between the two spectra is shown as the shaded area (inset shows the pulse sequence pump−deplete−probe). (b) Signal of S_1, relative to the pump−deplete delay T. Fit with monoexponential rise and decay, convoluted with the pump−deplete cross-correlation (solid curve).

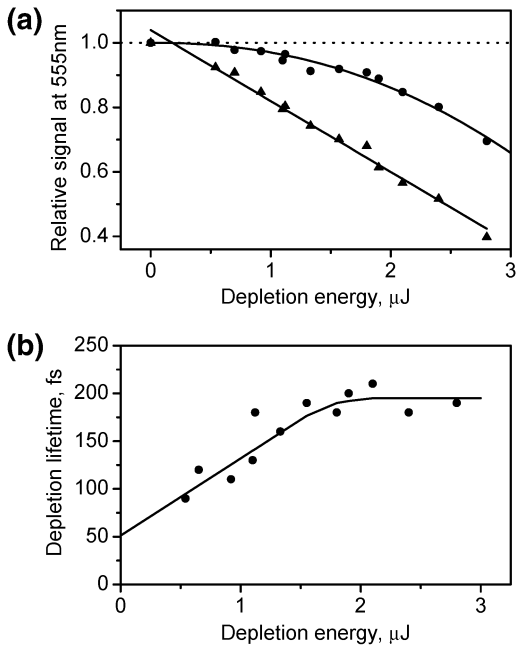

Figure 7. Energy dependence of depletion curves from zeaxanthin: (a) remnant signal of S_1 for two pump−deplete delay (T) values ((▲) at peak effect, with a linear fit, and (●) at 1 ps, with a power law fit proportional to $E^{2.3\pm0.6}$) and (b) lifetime of the depletion peak from fits to curves similar to that in Figure 6b. The line is a guide to the eye. Maximal power is 1.3×10^{16} photons/cm^2.

et al.[24]). Therefore, it seems reasonable that the short-lived state, which absorbs the depletion pulse at 795 nm, is the initially populated state, S_2 ($1B_u^+$). Our analysis focuses on the peak depletion signal and ignores the residual asymptotic depletion at longer delays, when S_2 is decayed. We attribute this small signal to nonresonant depletion directly from the S_1 state, possibly enhanced by the blue wing of the S_1-S_2 band.[25]

The observed energy dependence can be explained by wavepacket motion on a single potential energy surface between 20 and 195 fs. The former time (20 fs) is the error on zero offset in Figure 6b, and the latter time (195 fs) is the upper limit of Figure 7b, which is identified with the passing of the intersection to the lower surfaces. By increasing the depletion power, we can follow the molecule deeper into its distortion away from the Franck−Condon window. This view is supported by the theory of strong vibronic interaction between S_2 and S_1.[14] By comparing the S_2-S_1 internal conversion of various conjugation lengths, Fuss et al.[18] concluded that the relevant conical intersection is reached by symmetry distortion along the coupling coordinate of b_u angle-alternation modes.[18] Without symmetry deformation, $1B_u^+$ and $2A_g^-$ do not couple/convert at all[14] and, therefore, the molecule must deform by excursion along b_u modes. This excursion leads away from the plane of Franck−Condon active "tuning" coordinates[14] composed of a_g C=C stretch modes. The same picture is extracted from time-wavelength resolved fluorescence experiments on neurosporene ($N = 9$).[17] Within the fluorescence lifetime, the shape of the fluorescence spectrum changes and is attributed to the changing relative weight of the contributing vibrational modes. The Franck−Condon active modes couple to others within 40 fs, whose relaxation within 210−260 fs mixes with the 250-fs internal conversion.[17]

Our observation of a single electronic state contradicts the previous assumption that the near-IR absorption is initially generated by S_2 and ~100 fs later by some dark state ($1B_u^-$ or $3A_g^-$) after internal conversion;[8] no such time scales are observable. Another proposal was that S_2 is responsible only for the very early visible absorption and decays in just 10 fs to dark states that absorb in the near-IR region.[9] Of course, within our instrument response, we cannot exclude a 10-fs offset from time zero. However, there is the major disaccord with the fluorescence lifetime: 10 fs versus 195 fs. Intensity borrowing has been invoked to explain fluorescence from a dark state; however, this process should also allow absorption to this no-longer-dark state, and none is observed, even at low temperatures.[26]

We maintain that the fluorescing state—and, hence, also the near-IR absorbing state—is S_2. We thus reconcile the various observations of very fast absorption[9] and fluorescence[17] spectral dynamics, as well as the energy-dependent depletion window as three manifestations of "sidewards" motion on the S_2 potential energy surface along the coupling coordinates of internal conversion.

Discussion of S_{sol}*. If, indeed, the depletion resonance is absorption from the initially excited S_2 state, then S_{sol}*, which is not dependent on it, cannot be an excited state. Any excited state must be populated by deactivation of S_2 but the S_{sol}* signal does not seem to correlate with the initial excited population in S_2. Hence, we take a closer look at the model presented in (Figure 2d). This hot ground-state model is entirely consistent with the depletion experiments. There is no transition at 795 nm from the ground state; therefore, it should not be affected by the depletion pulse. The major question is how the hot ground state can be populated within the pump pulse duration. Any relaxation effects to or within the ground state would be too slow to explain a rise time that is very fast or instantaneous. However, one effect is, in fact, inevitable with femtosecond pulses: impulsive Raman scattering.[27,28] An ultrashort pulse with its corresponding broadband spectrum contains both "pump" and red-shifted "Stokes" frequencies of a Raman transition to

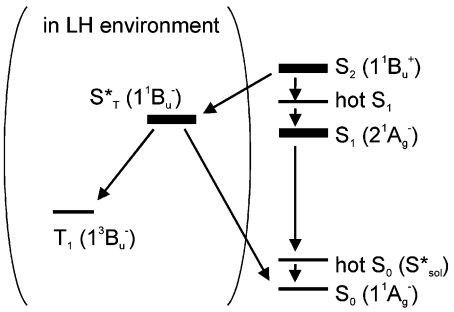

Figure 8. Unified model of carotenoids. States with thick levels contribute to excitation energy transfer inside light-harvesting (LH) complexes. Both S* signals absorb at the lower-energy side of the ground-state absorption. The S_T* ($1B_u^-$) channel is activated by external symmetry deformation and does not participate in solution. The S* signal in solution is the Raman-excited ground-state S_{sol}* = hot $S_0 \neq S_T$*.

higher vibrational modes. In our case, the laser is additionally electronically resonant, such that the Raman excitation is enhanced by up to six orders of magnitude.[29] Also, because of the shift of the potential minima, the Franck−Condon factors are higher for transitions from the initially excited S_2 without C=C stretch excitation to S_0 in higher quanta of the stretch modes. In fact, the S_{sol}* absorption matches the fluorescence spectrum of S_2-S_0 surprisingly well, peaking at 532 nm.[24] We propose that S_{sol}* is populated by impulsive Raman scattering of the pump pulse, enhanced by its electronic resonance (see Figure 2d). Internal conversion of S_1-S_0 additionally populates the vibrationally hot ground state, possibly leading to modes[30] other than the Raman-active modes populated by the impulsive Raman mechanism (see Figure 2d). Thus, S_{sol}* will live at least as long as S_1. This naturally explains the observation of the S_1 lifetime in this region for $N < 11$ and the constant lifetime of 6.2 ± 0.4 ps from the ground-state vibrational relaxation for longer N, as measured in Figure 4.

S_{sol}* and the newly found singlet excited state in LH complexes (S_T*) display approximately the same spectral profiles and comparable lifetimes, and yet they cannot be identical. When comparing the ratio of signal amplitudes, we notice that S_T^*/S_1 in LH2 is 80% higher than S_{sol}^*/S_1 in solution.[12] It is thus possible that, in LH2, the S_{sol}* signal is hidden by the stronger overlapping S_T* signal. In that case, the internal conversion from S_2 to S_T* would open up only in the non-C_{2h} geometry of a carotenoid that is distorted by geometric constraints of the LH complex,[31] which leads to an environment-dependent deactivation network (Figure 8).

5. Conclusion

Here, we presented pump−deplete−probe and transient absorption spectroscopy on $N = 11$ carotenoids in solution. The near-IR bands of the S_2 state were used as the depletion resonance. The experiments showed that the signal S_{sol}* is not identical to S_1 ($2A_g^-$) and cannot be assigned to an electronic excited state, because it does not suffer from depletion of the initially excited S_2 ($1B_u^+$) state. The lifetime of S_{sol}* is constant at 6.2 ± 0.4 ps for all carotenoids with $N \geq 11$, and, for $N < 11$, it matches the lifetime of S_1. We attribute S_{sol}* = hot S_0 to the Raman-excited ground state, populated by impulsive Raman scattering of the pump pulse and decaying by vibrational relaxation. Evidence was presented for motion on the S_2 potential energy surface toward electronic degeneracy along asymmetric coupling modes that would also result in spectral dynamics in fluorescence and absorption without the involvement of intermediate dark states.

Acknowledgment. We gratefully acknowledge generous support and continuous encouragement by Karl-Ludwig Kompa. The authors thank Tomáš Polívka for stimulating discussion about the nature of the near-IR bands and for the zeaxanthin samples.

References and Notes

(1) Christensen, R. L. The Electronic States of Carotenoids. In *The Photochemistry of Carotenoids*; Frank, H. A., Young, A. J., Britton, G., Cogdell, R. J., Eds.; Kluwer Academic Publishers: Dordrecht, The Netherlands, 1999; pp 137−157.

(2) Englman, R.; Jortner, J. *Mol. Phys.* **1970**, *18*, 145−164.

(3) Andersson, P. O.; Bachilo, S. M.; Chen, R.-L.; Gillbro, T. *J. Phys. Chem.* **1995**, *99*, 16199−16209.

(4) Frank, H. A.; Josue, J. S.; Bautista, J. A.; van der Hoef, I.; Jansen, F. J.; Lugtenburg, J.; Wiederrecht, G.; Christensen, R. L. *J. Phys. Chem. B* **2002**, *106*, 2083−2092.

(5) Frank, H. A.; Desamero, R. Z. B.; Chynwat, V.; Gebhard, R.; van der Hoef, I.; Jansen, F. J.; Lugtenburg, J.; Gosztola, D.; Wasielewski, M. R. *J. Phys. Chem. A* **1997**, *101*, 149−157.

(6) Tavan, P.; Schulten, K. *J. Chem. Phys.* **1986**, *85*, 6602−6609.

(7) Furuichi, K.; Sashima, T.; Koyama, Y. *Chem. Phys. Lett.* **2002**, *356*, 547−555.

(8) Fujii, R.; Inaba, T.; Watanabe, Y.; Koyama, Y.; Zhang, J. P. *Chem. Phys. Lett.* **2003**, *369*, 165−172.

(9) Cerullo, G.; Polli, D.; Lanzani, G.; De Silvestri, S.; Hashimoto, H.; Cogdell, R. J. *Science* **2002**, *298*, 2395−2398.

(10) Andersson, P. O.; Gillbro, T. *J. Chem. Phys.* **1995**, *103*, 2509−2519.

(11) Gradinaru, C. C.; Kennis, J. T. M.; Papagiannakis, E.; van Stokkum, I. H. M.; Cogdell, R. J.; Fleming, G. R.; Niederman, R. A.; van Grondelle, R. *Proc. Natl. Acad. Sci., U.S.A.* **2001**, *98*, 2364−2369.

(12) Wohlleben, W.; Buckup, T.; Herek, J. L.; Cogdell, R. J.; Motzkus, M. *Biophys. J.* **2003**, *85*, 442−450.

(13) Papagiannakis, E.; Kennis, J. T. M.; van Stokkum, I. H. M.; Cogdell, R. J.; van Grondelle, R. *Proc. Natl. Acad. Sci. U.S.A.* **2002**, *99*, 6017−6022.

(14) Domcke, W.; Stock, G. *Adv. Chem. Phys.* **1997**, *100*, 1−163.

(15) Li, J.; Woywod, C. *Chem. Phys. Lett.* **2003**, *372*, 128−138.

(16) Yan, M.; Rothberg, L.; Callender, R. *J. Phys. Chem. B* **2001**, *105*, 856−859.

(17) Akimoto, S.; Yamazaki, I.; Takaichi, S.; Mimuro, M. *Chem. Phys. Lett.* **1999**, *313*, 63−68.

(18) Fuss, W.; Haas, Y.; Zilberg, S. *Chem. Phys.* **2000**, *259*, 273−295.

(19) Billsten, H. H.; Zigmantas, D.; Sundstrom, V.; Polívka, T. *Chem. Phys. Lett.* **2002**, *355*, 465−470.

(20) Onaka, K.; Fujii, R.; Nagae, H.; Kuki, M.; Koyama, Y.; Watanabe, Y. *Chem. Phys. Lett.* **1999**, *315*, 75−81.

(21) Buckup, T.; Savolainen, J.; Wohlleben, W.; Hashimoto, H.; Herek, J. L.; Correira, R.; Motzkus, M., to be published, 2004.

(22) Macpherson, A. N.; Gillbro, T. *J. Phys. Chem. A* **1998**, *102*, 5049−5058.

(23) Getoff, N. *Rad. Res.* **2000**, *154*, 692−696.

(24) Kandori, H.; Sasabe, H.; Mimuro, M. *J. Am. Chem. Soc.* **1994**, *116*, 2671−2672.

(25) Polivka, T.; Zigmantas, D.; Frank, H. A.; Bautista, J. A.; Herek, J. L.; Koyama, Y.; Fujii, R.; Sundström, V. *J. Phys. Chem. B* **2001**, *105*, 1072−1080.

(26) Christensen, R. L.; Goyette, M.; Gallagher, L.; Duncan, J.; DeCoster, B.; Lugtenburg, J.; Jansen, F. J.; van der Hoef, I. *J. Phys. Chem. A* **1999**, *103*, 2399−2407.

(27) Yan, Y.-X.; Gamble, E. B.; Nelson, K. A. *J. Chem. Phys.* **1985**, *83*, 5391−5399.

(28) Weiner, A. M.; Leaird, D. E.; Wiederrecht, G. P.; Nelson, K. A. *Science* **1990**, *247*, 1317−1319.

(29) Albrecht, A. C. *J. Chem. Phys.* **1961**, *34*, 1476−1484.

(30) Siebert, T.; Maksimenka, R.; Materny, A.; Engel, V.; Kiefer, W.; Schmitt, M. *J. Raman Spectrosc.* **2002**, *33*, 844−854.

(31) McDermott, G.; Prince, S. M.; Freer, A. A.; Hawthornthwaite-Lawless, A. M.; Papiz, M. Z.; Cogdell, R. J.; Isaacs, N. W. *Nature* **1995**, *374*, 517−521.